

Single-Mode Lasing Operation Using a Microring Resonator as a Wavelength Selector

Seoijin Park, Seong-Soo Kim, Liwei Wang, and Seng-Tiong Ho

Abstract—We have demonstrated semiconductor lasers with microring resonators as frequency-selective elements. We show that the small resonator inside the laser makes single frequency-mode operation possible with reasonably good side-mode rejection.

Index Terms—Etching, microring resonators, plasma materials-processing applications, quantum wells, semiconductor lasers, waveguides.

I. INTRODUCTION

MICRORING resonators are proving to be good candidates for use in very large-scale integrated (VLSI) photonic circuits such as channel dropping filters, WDM demultiplexers, and wavelength space switches [1]–[4]. The main advantage that microring resonators have is the large free spectral range of resonance arising from their small cavity size. A free spectral range of 10–42 nm can be achieved with 20–5- μm diameter ring resonators.

In this paper, we show that a passive microring resonator can be used as a frequency selective element to achieve single frequency lasing in semiconductor lasers. We believe that this is the first demonstration of what we call passive microring resonator-based lasers (PMR-based lasers). We show that it is possible to obtain single-frequency lasing with a 20 μm diameter passive ring resonator in a 2-mm-long linear cavity. This PMR-based laser also shows good side-mode rejection and has a reasonably low threshold current. Note that this kind of laser is different from a microring cavity laser for which the ring cavity itself is both gain medium and resonator. Here, we take advantage of the large free spectral range of a small microring structure together with the long gain length to achieve high-power single-mode lasing. Separation of the passive ring cavity from the active medium allows us to tune the ring resonator frequency independently so that it is not affected by heating or other effects arising from the injection current. Furthermore, we show that by having the active medium in the ring resonator to be the same as that in the linear cavity, we can engineer the ring resonator

Manuscript received April 4, 2001; revised November 29, 2001. This work was supported by National Science Foundation under Grants DMR-9632472 and ECS-9502475 and by DARPA under Grant F49620-96-1-0262/P006.

S. Park was with the Department of Electrical and Computer Engineering, Northwestern University, Evanston, IL 60208-3112 USA. He is now with Sarnoff Corporation, Princeton, NJ 08540 USA.

S.-S. Kim is with the Department of Physics and Astronomy, Northwestern University, Evanston, IL 60208 USA.

L. Wang was with the Department of Electrical and Computer Engineering, Northwestern University, Evanston, IL 60208-3112 USA. He is now with the Lightcross Corporation, Pasadena, CA 91101 USA.

S.-T. Ho is with the Department of Electrical and Computer Engineering, Northwestern University, Evanston, IL 60208-3112 USA.

Publisher Item Identifier S 0018-9197(02)01757-8.

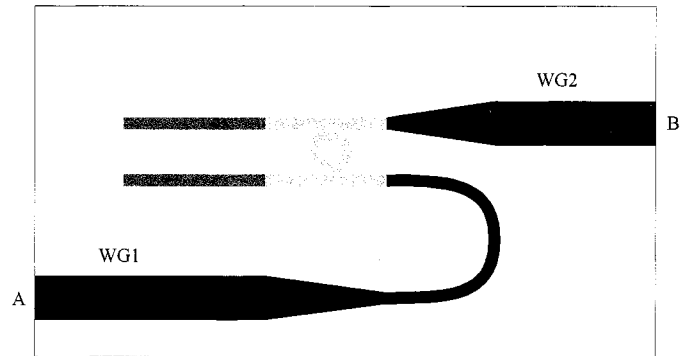


Fig. 1. Schematic diagram of a PMR-based laser. The black, light-gray, and dark-gray colors represent active, transparent, and absorption regions, respectively.

to have one dominant transmission frequency, leading to robust single frequency lasing. These results arise from a combination of the wide resonant frequency spacing of the ring resonator and the substantial enhancement of the peak of the gain curve. Our PMR-based laser is quite different from coupled cavity lasers which have inherent instability problems associated with their sub-cavities. The PMR laser uses a microring resonator as a purely transmission style wavelength selector, eliminating any problems associated with sub-cavities within the main laser cavity.

II. DEVICE STRUCTURE AND FABRICATION

The device structure we have fabricated is shown in Fig. 1, where a small ring resonator is inserted into a conventional Fabry–Perot laser. In this figure, the black region is actively pumped by injection current to achieve gain, and the light-gray region is separately pumped by injection current to achieve transparency. We used ring resonator designs with diameters of 5, 10, and 20 μm to give free spectral ranges of 42, 21, and 10.5 nm, respectively. These free spectral ranges are designed to be large enough so that only one mode is situated around the peak of the gain spectra. In Fig. 1, waveguide 1 (WG1) and waveguide 2 (WG2) have cleaved facets A and B which act as the output ends of the cavity. Light at the microring resonant frequency will couple into the resonator and travel between waveguide 1 and 2 through the resonator. Light that is off the microring resonant frequency will not be able to do so. Suppose we follow light at the resonant frequency, beginning at cleaved facet A, propagating toward the resonator through waveguide 1. This light beam, after crossing the resonator, will reflect back at cleaved facet B, and cross the resonator again. After that, it will reflect back at the cleaved facet A, and then constructively

interfere with the beginning beam to form a standing wave. The optical cavity mode formed by this closed path will be referred to as the W–R–W (waveguide–resonator–waveguide) cavity mode. Let us now follow light not at the resonance frequency. This light, beginning at facet A, will pass by the resonator and continue to propagate toward the other unclefted end of waveguide 1. If this light is reflected back strongly from the unclefted end, an optical cavity will be formed. To prevent the two facets of waveguide 1 and 2 from forming Fabry–Perot cavities (which we will call the W_1 and W_2 cavities), the unclefted ends of waveguide 1 and 2 should either be etched with a rough pattern to drastically reduce reflection, or filled with an absorber. In our case, an absorption section is situated between the resonator and the unclefted end of the waveguide for both waveguide A and B. This absorption section is shown as the dark-gray region in Fig. 1.

The devices reported here were fabricated from a particular layer structure of InGaAsP grown epitaxially on an InP substrate with lattice matching. The layer structure comprises an InP substrate, an n-doped region, an InGaAsP-graded barrier region, a quantum-well region, and a p-doped region. The n-doped region consists of a 30-nm-thick InGaAsP buffer layer ($\lambda = 1.1 \mu\text{m}$, $n = 1 \times 10^{18}/\text{cm}^3$) and a $1.6 \mu\text{m}$ n-doped InP cladding layer ($n = 5 \times 10^{17}/\text{cm}^3$) separated by an n-type InP buffer layer with a dopant density of $n = 1 \times 10^{18}/\text{cm}^3$ from the InP substrate. The graded barrier region follows the n-doped region. It has 70 nm of InGaAsP ($\lambda = 1.08 \mu\text{m}$), 70 nm of InGaAsP ($\lambda = 1.16 \mu\text{m}$), and 30 nm of InGaAsP ($\lambda = 1.25 \mu\text{m}$) successively. The quantum well is situated between the graded barrier region and the top p-doped region. The quantum well consists of four 9-nm InGaAs quantum wells separated by three 22-nm InGaAsP ($\lambda = 1.25 \mu\text{m}$) layers. The top p-doped region consists of a $0.5\text{-}\mu\text{m}$ p-doped InP cladding layer ($p = 3 \times 10^{17}/\text{cm}^3$), a 20-nm p-doped InGaAsP layer ($\lambda = 1.3 \mu\text{m}$, $p = 1 \times 10^{18}/\text{cm}^3$), a $0.5\text{-}\mu\text{m}$ p-doped InP cladding layer ($p = 5 \times 10^{17}/\text{cm}^3$), a 20-nm p-doped InGaAsP layer ($\lambda = 1.3 \mu\text{m}$, $p = 1 \times 10^{18}/\text{cm}^3$), a $0.6\text{-}\mu\text{m}$ p-doped InP cladding layer ($p = 5 \times 10^{17}/\text{cm}^3$), and a $0.1\text{-}\mu\text{m}$ p-doped InGaAsP cap layer ($\lambda = 1.3 \mu\text{m}$, $p = 1 \times 10^{19}/\text{cm}^3$). In order to fabricate microring lasers coupled to submicron-wide waveguides (nanoscale waveguides), a negative NEB-22 e-beam resist was spun at 380-nm thickness onto a 400-nm-thick SiO_2 mask and patterned with a Leica EBPG-4 direct e-beam writer. The NEB-22 resist was then developed using a Shipley MF 319 developer. The area not written by the e-beam was dissolved, unlike the usual PMMA (positive) resist. The waveguide width of the microring resonators and the coupled waveguides was $0.4 \mu\text{m}$. The gaps between the microring resonators and the coupled waveguides were set to be $0.2 \mu\text{m}$. We then patterned ring diameters of 5, 10, and $20 \mu\text{m}$. The coupled waveguides were gradually expanded out to $2 \mu\text{m}$ with a $200\text{-}\mu\text{m}$ transition region. We used proximity correction to correctly develop the $0.2\text{-}\mu\text{m}$ gap between the coupled waveguides and the microring resonators. After developing the patterned e-beam resist, a SiO_2 mask was etched down using RIE with 31/6 sccm CF_4/H_2 plasma, at 100 W of RF power, 289-V dc bias, and 30 mTorr. The wafer covered by the patterned SiO_2 mask was then etched using ICP with 10/35/10 sccm $\text{Cl}_2/\text{N}_2/\text{Ar}$ plasma at 140 W ICP power, 354-V dc bias, 2.3 mTorr pres-

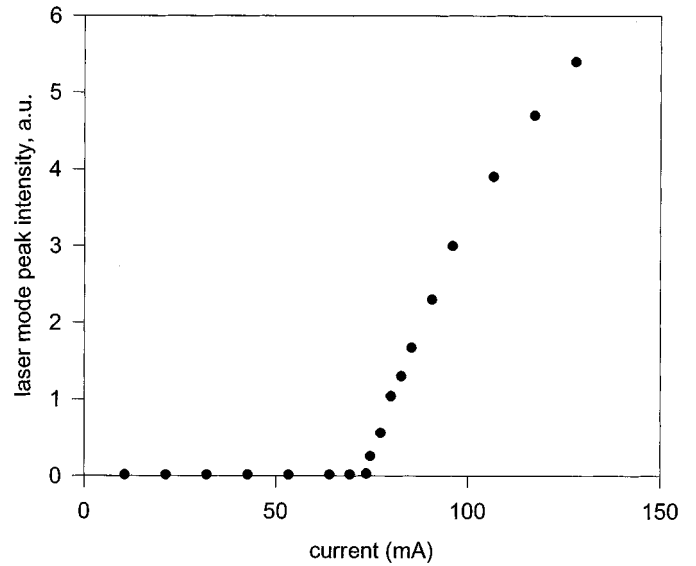


Fig. 2. Experimental plot of light versus current characteristic of the PMR-based laser. Lasing characteristic.

sure, and $250 \text{ }^\circ\text{C}$ temperature. In order to make a clear gap between the coupled waveguide and the resonator, the gap region was etched down to a depth of $3 \mu\text{m}$. However this resulted in a $5\text{-}\mu\text{m}$ etching depth for the relatively wide open waveguide area due to the etching rate difference between the narrow gap region and the widely open region. The effective gap size obtained at the narrow gap region is less than $0.2 \mu\text{m}$ due to the slope of the etched profile around the gap region. In order to fill the gaps in the etched region planarization processes followed the etching processes that had formed the microring resonators and the waveguides. First we deposit $1\text{-}\mu\text{m}$ -thick SiO_2 using PECVD before filling the opening area with benzocyclobutene (BCB). The BCB was spin-coated to a thickness of $5 \mu\text{m}$ to fill the gaps, and then baked at $300 \text{ }^\circ\text{C}$ for 30 mins. The baked BCB was etched down to the waveguide top surface using RIE with a 10/30 sccm CF_4/O_2 plasma at 150-W RF power, 273-V dc bias, and 100 mTorr. Photolithography was then carried out to open the window and remove the SiO_2 on the top of the waveguides. After removing the SiO_2 on the top of the waveguides and making a photoresist pattern for electrodes, 400/300/5000-nm Ti/Pt/Au metal layers were deposited and lifted off to form the p-side contact, and 800/200/4000-nm AuGe/Ni/Au metal layers were deposited on the back of the substrate to form the n-side contact. The fabricated chips were then cleaved to obtain W–R–W Fabry–Perot cavities long enough to avoid a mismatch between the resonant frequency modes of the ring resonator and the W–R–W resonator. This is achieved with a cleaved length of around 2 mm. The 2-mm-long W–R–W Fabry–Perot cavity has a free spectral range of about 0.2 nm. Thus, the lengths of waveguides 1 and 2 are about 1-mm long.

III. RESULTS AND DISCUSSION

Fig. 2 shows the lasing characteristics of the PMR-based laser, where data were taken from the lasing peak in the emission spectrum, and the laser was pumped with $5\text{-}\mu\text{m}$ -long electrical pulses at $95\text{-}\mu\text{s}$ intervals. The current in the ring

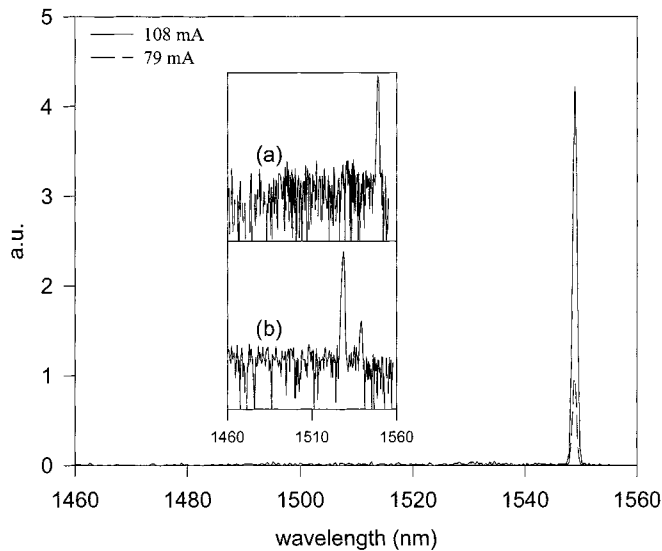


Fig. 3. Lasing spectra of the PMR-based laser. Insets (a) and (b) show the lasing spectra of the PMR-based laser and a 20- μ m-diameter microring laser with 8- μ m-wide waveguide, respectively.

resonator is set to be around 0.4 mA, a level low enough that the ring resonator did not lase. The threshold current was around 70 mA, corresponding to a 1.75 kA/cm² current density. When we brought the current from threshold up to a value of 140 mA, well above the lasing threshold, no mode hopping was observed throughout this entire current range. In Fig. 3, we show the emission spectra of the laser with 79 and 108 mA injected currents. The lasing wavelength of the devices is located around 1.549 μ m. In the emission spectra, the side-mode peaks of the ring resonator are not clearly visible. The intensities of the side modes may be too small to be distinguished from the noise levels. The lasing wavelength of the PMR-based laser is around the calculated $n = 1$ exciton level (1.55 μ m). This shows that the lasing wavelength of the PMR-based laser is at the first ring resonance wavelength next to the $n = 1$ exciton level. In the insets of Fig. 3, the lasing spectrum of the PMR-based laser [inset (a)] is compared with that of a microring laser [inset (b)] that was fabricated using the same wafer with a 0.8- μ m waveguide width and 20- μ m ring diameter. In this inset, an arbitrary logarithmic intensity scale is used. From the inset, we see that the microring laser has two resonant modes at wavelengths shorter than that of the PMR-based laser, along with clear side-mode excitations. Furthermore, the threshold current density of the microring laser is found to be 2.28 kA/cm², which is higher than that of the PMR laser.

These phenomena result from three effects. First, side longitudinal modes are suppressed by the gain spectra. Generally, side longitudinal modes are more suppressed as the ratio of the gain spectral range of the laser to the free spectral range of the laser cavity is reduced [5]. Second, the gain peak shifts. As the threshold carrier density increases, the gain spectral range becomes wider and the gain peak shifts to shorter wavelengths. Thus, the gain spectral range of the PMR-based laser is expected to be narrower than that of the microring laser. The gain peak of the PMR-based laser will be located at longer wavelengths as

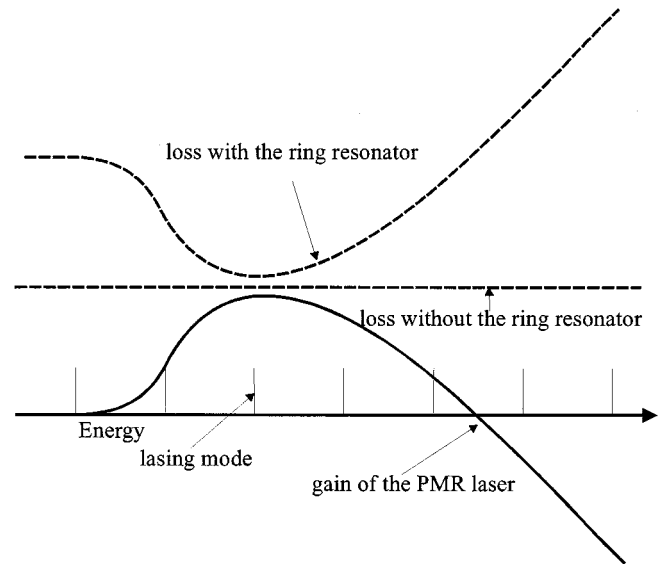


Fig. 4. Schematic illustration of the longitudinal-mode spectrum of the ring resonator, its dependence on the gain spectrum, and the optical loss from the transmission through the resonator.

well. However, the above effects are not sufficient to explain the effective side-mode suppression of the PMR-based laser. This is because, unless the gain spectral range of the laser is so narrow that it contains only one longitudinal mode, the side modes next to the lasing mode should be observable just as in the case of the microring laser. As the required narrow-gain spectral range seems to be unrealistic with the large threshold current density of the PMR laser, we need to look for an additional explanation.

In addition to the high ratio of FSR of the ring resonator to gain spectral range (or the small number of longitudinal modes with positive gain), the side longitudinal modes in the PMR-based laser seem to be additionally suppressed by the lower transmissions of the side modes through the ring resonator. The carrier density of the ring resonator is controlled separately in the PMR-based laser. Therefore, the transmission of the resonance modes of the ring resonator can be controlled separately through current injection into the ring resonator. At the current injection level where the gain peak is located around the $n = 1$ exciton level, the resonant transmission through the ring resonator itself in the PMR-based laser decreases as the resonance wavelength is more distant from the exciton level. Transmission of these resonance modes is determined by the gain values of the modes. Thus, the transmission of the mode around the gain peak will be much higher than that of the next mode in the absorption. From this reasoning, we see that the lasing mode of the PMR-based laser is determined not only by the PMR-based laser gain, but also by the ring resonator transmission. In this experiment, the current density of the ring resonator is tuned close to the threshold current density of the PMR-based laser and is at 1.62 kA/cm². This means that the gain curve of the ring resonator is close to that of the PMR-based laser (which will be clamped at the threshold level), as is the location of the peak gain of the ring resonator. Therefore, among the resonant modes, the lasing mode would have the highest gain and the lowest optical loss through the ring resonator, as shown in Fig. 4. If so, the side-mode suppression can be significantly larger be-

cause of the mixed effect of the gain and transmission through the ring resonator, and so the intensities of the side modes can be negligible as observed in this experiment. Since we did not observe any other resonant peaks in the emission spectrum or mode hopping, we can say that high purity single-mode lasing is possible in the PMR laser structure. In Fig. 3, the peak intensity in the lasing spectrum of PMR laser is 22-dB above the spontaneous emission background and the spontaneous emission is pinned at the threshold level when the current is above threshold. Therefore, the degree of single-mode lasing can be expected to increase as the lasing peak intensity increases.

In addition to the above effects, in the microring lasers, current-induced heating can cause various problems at high current density. These problems include decreasing the laser output, shifting of the lasing wavelength, and the line width broadening. Such current induced heating problems are important in microring lasers because they require higher threshold current densities. Their small volumes also make heat dissipation less efficient. In microring lasers, this heat-generating microring serves as a resonant cavity, which results in the shifting of the resonance wavelength. In contrast, the PMR-based lasers are free of such current-induced heating effects. The lasing wavelength of the PMR-based laser is uniquely determined by the resonator, which does not require as much current density as the microring laser. As long as the current injection into the resonators is not changed, the lasing wavelength is very stable as shown in Fig. 3. Unlike the microring laser, the ring resonator in the PMR-based laser is not part of the laser gain medium. Hence, only the transmission of the ring resonator affects the threshold current density. Therefore, the PMR lasers are almost free of the current-induced heating problems.

Besides the 20- μm PMR-based lasers described above, we also measured PMR lasers with 10- and 5- μm diameter ring resonators. However, lasing was not observed, possibly because of the lower coupling efficiency or the higher optical loss of the smaller ring resonators.

IV. CONCLUSION

We have demonstrated semiconductor lasers using microring resonators as frequency selective elements. With a small enough resonator inside the laser, single frequency mode operation was obtained with reasonably good side-mode rejection. The laser utilizes the large free spectral range of the microring structure together with the advantage of a long gain length to achieve high-power single-mode lasing. We found that side longitudinal-mode suppression can be enhanced for better single-mode lasing purity with gain control in the ring resonator separate from that in the active laser medium. This separate control also makes the laser immune to some undesirable effects at high output power, such as a shift in the lasing wavelength and linewidth broadening from current heating inside the laser gain medium.

REFERENCES

- [1] S. T. Chu, B. E. Little, W. Pan, T. Kaneko, S. Sato, and Y. Kokubun, "An eight-channel add-drop filter using vertically coupled microring resonators over a cross grid," *IEEE Photon. Technol. Lett.*, vol. 11, pp. 691–693, 1999.
- [2] B. E. Little, H. A. Haus, J. S. Foresi, L. C. Kimberling, E. P. Ippen, and D. J. Ripin, "Wavelength switching and routing using absorption and resonance," *IEEE Photon. Technol. Lett.*, vol. 10, pp. 816–818, 1998.
- [3] B. E. Little, S. T. Chu, W. Pan, and Y. Kokubun, "Microring resonator arrays for VLSI photonics," *IEEE Photon. Technol. Lett.*, vol. 12, pp. 323–325, Mar. 2000.
- [4] D. Rafizadeh, J. P. Zhang, S. C. Hagness, A. Taflove, K. A. Stair, and S. T. Ho, "Waveguide-coupled AlGaAs/GaAs microcavity ring and disk resonators with high finesse and 21.6-nm free spectral range," *Opt. Lett.*, vol. 22, pp. 1244–1246, 1997.
- [5] T. P. Lee, C. A. Burrus, J. A. Copeland, A. G. Dentai, and D. Marcuse, "Short-cavity InGaAsP injection lasers: dependence of mode spectra and single-longitudinal-mode power on cavity length," *IEEE J. Quantum Electron.*, vol. QE-18, pp. 1101–1113, 1982.

Seojin Park was born in Seoul, Korea, in 1964. He received the B.S. and M.S. degrees from Yosei University, Seoul, Korea, in 1987 and 1989, respectively, and the Ph.D. degree in electrical and computer engineering from Northwestern University, Evanston, IL, in 2000.

He is currently with Princeton Lightwave, Cranbury, NJ, as a Senior Researcher. His research interests are in the design and development of photonic integrated circuits for fiber-optic communication systems.

Seong-Soo Kim was born in Korea in 1966. He received the B.S. degree from Inha University, Incheon, Korea, in 1990 and the M.S. degree from Northwestern University, Evanston, IL, in 1994, both in physics. He is currently working toward the Ph.D. degree in the Department of Physics and Astronomy, Northwestern University.

His research interests are in integrated photonic devices, including microring resonator-based semiconductor lasers, nonlinear optical waveguide devices, and high-speed electrooptic modulators.

Liwei Wang was born in Shandong, China, in 1964. He received the B.A. degree from Tsinghua University, Beijing, China, in 1987, and the Ph.D. degree in physics from the University of Rochester, Rochester, NY, in 1993.

He then joined Northwestern University, Evanston, IL, performing post-graduate work in integrated photonics. Currently, he is with LightCross, Inc., Monterey Park, CA.

Seng-Tiong Ho (S'83–M'89) received the B.S., M.S., and Ph.D. degrees in electrical engineering from the Massachusetts Institute of Technology, Cambridge, in 1984 and 1989, respectively.

From 1989 to 1992, he was a Member of Technical Staff at AT&T Bell Laboratories, Murray Hill, NJ. Since 1991, he has been a Faculty Member in the Department of Electrical and Computer Engineering, Northwestern University, Evanston, IL. His research areas include microcavity lasers, quantum phenomena in low-dimensional photonic structures, nanofabrication, ultrafast nonlinear optical phenomena, electrooptic modulators, optical communications, and quantum optics.

Dr. Ho is a member of Phi Beta Kappa, Tau Beta Pi, Sigma Pi Sigma, and Sigma Xi.